

Full Length Research Paper

Geographic information system (GIS) and remote sensing for multi-temporal analysis of sand encroachment at Oglet Merteba (South Tunisia)

Dalel OUERCHEFANI^{1*}, Hanen DHAOU¹, Eric DELAITRE², Yann CALLOT³ and Saadi ABDELJAOUED⁴

¹Institut des Régions Arides, 22 km route Jorf, 4119, Medenine, 22 km route Jorf, 4119, Medenine, Tunisia.

²Institut de Recherche pour le Développement, 911 avenue Agropolis, BP 64501, 34394 Montpellier cedex 5, France.

³Faculté de Géographie, Histoire, Histoire de l'art, Tourisme, France.

⁴Faculté des Sciences Mathématiques, Physiques et Naturelles de Tunis, Tunisia.

Accepted 1 August, 2013

Sand encroachment in South Tunisia is one of the most serious environmental problems. Close to six decades, several irrational human activities are responsible for the increase in the magnitude of sand encroachment. They include overgrazing, denudation of vegetation cover and many other disturbances of the fragile arid ecosystem. Mapping this phenomenon is now essential for a better understanding of the general evolution of this process to setup and implement efficient protection techniques. The study done in the "Oglet Merteba" area was performed using the geographic information system (GIS) and remote sensing techniques particularly those referring to change detection. This kind of approach integrates direct and calculated environmental parameters in a geo-referenced data base, allowing the spatial and temporal analysis of the evolution of this phenomenon. The results show that despite the multiple efforts put together to control wind erosion, areas prone to wind erosion increased from 5 % in 1975 to 6.7% in 2006. The most important progression rate is noticed between 1987 and 2000.

Key words: South Tunisia, sand encroachment, geographic information system (GIS), remote sensing, change detection, progression rate.

INTRODUCTION

Land degradation is considered as one of the most important environmental problems linked to climatic variations and human activities in arid and semiarid regions (Adeel et al., 2005). This phenomenon defined as "a long-term loss in ecosystem function and productivity" (Bai and Dent, 2007) has concerned Tunisia since the second half of the twentieth century. Its symptoms include nutrient depletion, salinity, water scarcity, pollu-

tion, disruption of biological cycles, loss of biodiversity and soil erosion which is very critical especially in Southern Tunisia. This necessitates mapping of wind erosion and sand encroachment evolution to help decision makers to undertake better management plans against desertification and to adapt sustainable land use policies. Remote sensing and GIS technologies are very suitable for this kind of research because they provide

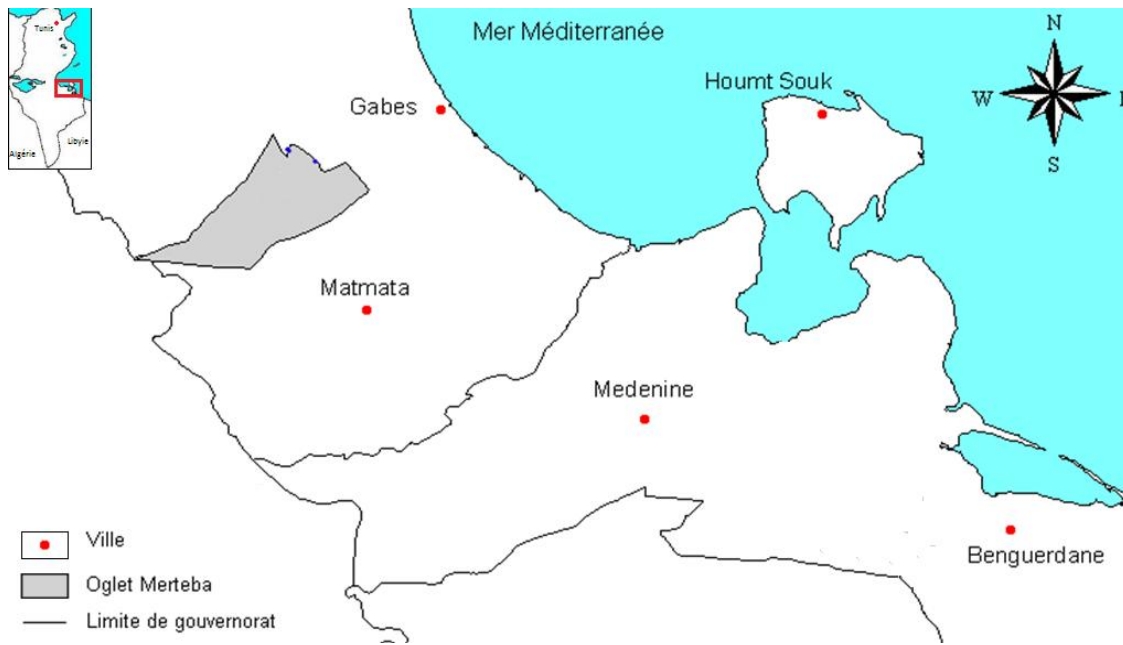


Figure 1. Study area of Oglet Merteba.

Table 1. Satellitary data used.

Acquisition date	Sensor	Spatial resolution
26 December 1975	MSS	80
18 June 1987	TM	30
10 April 2000	ETM+	30
10 March 2006	ETM+	30

up-to-date quantitative data and products at different spatial and temporal scales to generate practical indicators for environmental assessment and monitoring.

MATERIALS AND METHODS

Study area

The study area of Oglet Merteba is located in Southern Tunisia. It is situated in the natural region of Jeffara at about 35 Km far from Gabes in the east and Matmata in the south (Figure 1). In the west, it is confined by the Jebels Tebaga and Hallouga in the North-west.. The mean annual rainfall is 190 mm. The Oglet Merteba plain is essentially formed by clayey gypsy sandy soils of the Mio-Pliocene; the erosion of these soils in the mountains forms locally gypsy crusts in their glacis. In the middle of the plain, important sand deposits are encountered.

Vegetation is composed of chamephytic shrubs represented by gypsophyl and psamophyl species that cover 5 to 30% of the soil in spring season. During humid periods, the vegetation cover can reach 60% due to the development of annual vegetation. The land

is mostly used for grazing; thus 90 to 95% of the surface is reserved for sheep, goat and camel livestock that are concentrated around human habitations, creating overgrazing zones where others remain underexploited.

Data

Collection of available data was the first task to be accomplished and the acquisition of satellite images proved to be cumbersome. In fact, although old products are available for free download in many websites, the new data sets are not easy to access and quite expensive. For that reason only four satellite images were used for this study (Table 1). They have been downloaded from the USGS server (<http://www.glovis.usgs.gov>); the first was taken by the MSS sensor, the second by TM sensor and the last two images by the ETM+ sensor. These images belonging to the path 191 and row 37 cover an area of 185 km² for a period of 31 years. A number of other maps such as soil, land use and geology were also used to conduct this study.

Geometric correction of all spatial data

All maps were first corrected within the Universal Transverse Mercator projection, datum Carthage, to be digitized and integrated under a Geographic Information System. Then, the topographic map was used to correct geometrically the four satellite images.

Radiometric and atmospheric calibration of satellite images

The information provided by the satellite images is not comparable because of its purity. The signal given by each image is noisy as it is subject of many atmospheric effects essentially absorption and scattering. These effects have not the same intensity for images

depending on many factors in relation to climate conditions, nature of the sensor, geometric conditions in the moment of the acquisition (sun elevation, time, solar zenith angle, etc.). For these reasons, all the images were first radiometrically corrected converting their DN to radiance and were atmospherically corrected converting the radiance to surface reflectance (Ouaidrari and Vermote, 1999) (Equation 1).

The 6S model (Second Simulation of Satellite Signal in the Solar Spectrum) (Vermote et al., 1997) was used to eliminate the atmospheric and illumination effects. The minimum data set needed to run this model is the meteorological visibility, type of sensor, sun zenith and azimuth, date and time of image acquisition and latitude and longitude of scene center. Using the input data and the embedded features, the model produces variables for assessing the surface reflectance.

$$\rho_S = \frac{\rho_{int}}{1 + S_{R+A} \times \rho_{int}} \quad (1)$$

With

$$\rho_{int} = \frac{(C_{slope} \times DC - C_{offset}) \pi d^2 / E_S}{\mu_S T_{gO_3} T_{gO_2} T_{gH_2O} T_{R+A}} - \frac{\rho_{R+A}}{T_{gH_2O} T_{R+A}} \quad (2)$$

S is the Rayleigh and aerosol spherical albedo, DC is the TM digital count, C_{slope} and C_{offset} are the calibration coefficients used for converting DC to sensor radiance (W/m²/sr/m), E_S is the solar irradiance in TM channels, d is the distance between the Earth and the Sun (km), ρ_{R+A} is the atmospheric intrinsic reflectance (Rayleigh and aerosol), T_{gO_2} is the oxygen absorption transmittance, T_{gO_3} is the ozone absorption transmittance, T_{gH_2O} is the water vapor absorption transmittance, T_{R+A} is the Rayleigh and aerosol scattering transmittance, $\mu_S = 1/\cos(\theta_S)$

These procedures allow one to define for each element on the surface a spectral signature with meaningful units that can be compared from one image to another. This would be required where the area of study is larger than a single scene or if monitoring change at a single location with different images taken at different times. This is known as diachronic analysis. Atmospheric correction allows also building of libraries of spectral signatures containing lists of different objects or surfaces and their reflectance.

Change detection of sand encroachment over a period of 31 years

A wide range of techniques are available to detect changes from multi-temporal remote sensing data sets (Fung and Ledrew, 1987; Jensen et al., 1993; Deer, 1995; Jensen, 2004 and Lu et al., 2004). One of these methods, or the image differencing, is basically the subtraction of the pixel digital values of a first image from the corresponding pixel values of a second one captured in another date. The histogram of the resulting image shows a range of pixel values from negative to positive numbers, where those clustered around zero represent no change and those at either tail represent reflectance changes from one image date to the next (Hayes and Sader, 2001). This method has been documented widely in change detection research. Some investigators like this method because of its accuracy, simplicity in computation and easy interpretation.

According to the last authors, one difficulty encountered in using image differencing for change detection is the selection of the appropriate threshold values in the histogram that separates real and spurious change. The subjectivity of threshold definition depends on the analyst's familiarity with the study area as well as access to auxiliary data such as field information, GIS data, and/or

matching dates of aerial photography (Hayes and Sader, 2001). These thresholds were chosen based on the images corresponding to the Color Index (CI). In fact, previous studies showed that this index is efficient for characterizing soil erosion, detecting the existence of sand deposits and monitoring its horizontal evolution in the images (Escadafal, 1989; Escadafal et al., 1994; Ghram-Messedi and Delaitre, 2007; Bannari et al., 2007). It is important to notice that this Index is used only to detect the spatial distribution of sand and has no relation with the thickness of the deposits or their amounts. An integrated method was then adopted to map and determinate the change between two consecutive dates. The following steps were followed:

1. Generation of CI images calculated as:

$$CI = \frac{(R-G)}{(R+G)} \quad (3)$$

Where G and R are the green and red channels of a TM or ETM+ sensor. Low valued CIs have been shown to correlate with high concentration of carbonates or sulfates and higher values correlate with crusted soils and sands in arid regions (Escadafal, 1989; Escadafal and Huete, 1991; Mougnot and Cailleu, 1995; Mathieu et al., 1998).

2. Determination of regions of interests relative to "sand" on the last image, based on the "field reality" database that was generated during the last image acquisition year;
3. Defining the thresholds of CI relative to the 2 classes of "sand" and "other"
4. Segmentation of all the CI images on 2 classes "sand" and "other";
5. The difference image gives area of positive changes (progression), negative changes (regression) and no changes (stable).

To better understand the multi-temporal evolution of sand accumulation, 5 rates were calculated (Table 2), based on the progression (P) and regression (R) between two times t_1 and t_2 .

RESULTS

Wind erosion is dominant at Oglet Merteba where soil structure and texture and wind velocity coupled with its geomorphologic position make it a perfect wind corridor (Chahbani, 1992). In this region, sandy surfaces are generally in continuous increase for the entire time series (1975-2006) (Table 3). The area affected in 1975 and 1987 was 5% (Table 3) but it increased to a maximum of 6.8% recorded in 2000 and 6.7% in 2006. This soil degradation noticed between 1987 and 2000 at Oglet Merteba was also shown by using other radiometric indices (Normalized Difference Vegetation Index NDVI and Brightness Index BI) (Ouerchefani et al., 2009). Wind erosion dynamics is more pronounced between 1987 and 2000 during which an increase of 1.7% is calculated. Between 2000 and 2006, the annual rate of change is equal to 1.54%; the rate is almost equally divided between progression (0.77%) and regression (0.78%) (Table 4). It is as if the same amount of sand lost in the departure areas had accumulated in the new drop zones (Pontanier and Zante, 1976). The same is observed for

Table 2. Calculated rates for change characterization.

Rate	Expression	Meaning
Global change	$C_g = P_{t_2-t_1} + R_{t_2-t_1}$	Surface object of both changes: progression and regression
Annual change	$C_a = \frac{P_{t_2-t_1} + R_{t_2-t_1}}{t_2 - t_1}$	The mean global change calculated for one year in absolute value
Annual progression	$P_a = \frac{P_{t_2-t_1}}{t_2 - t_1}$	Surface object of only progression
Annual regression	$R_a = \frac{R_{t_2-t_1}}{t_2 - t_1}$	Surface object of only regression
Annual net progression	$P_{na} = P_a - R_a$	The mean global resulting change (could be negative)

Table 3. Sandy surfaces at Oglet Merteba.

Oglet Merteba	1975	1987	2000	2006
Area (ha)	2253.0	2298.0	3064.0	3019.0
Area (%)	5.0	5.1	6.8	6.7

the period 1975-1987, during which, the annual rate of change is calculated as 0.82%. 0.41% are newly affected areas in 1987 compared to 1975; while 0.41% of areas were not any more sandy.

The only review of annual net progression rate does not reflect the intensity of the wind dynamics. A low P_{na} may actually hide a very pronounced wind activity in both progression and regression. Sand progression and regression in Oglet Merteba are very local (Figure 2); they concern almost the same areas. Stable sand surfaces occupy a small area; they are located in the plain of Oglet Merteba and seem to evolve over the last map change near the village of Sidi Guenaou.

At Oglet Merteba, rates of change are in proportion with the number of wet years (Table 5). This correlation of weather conditions with soil degradation has been shown in many studies related to arid lands of Tunisia (Talbi, 1993; Jauffret, 2001). Floret and Pontanier (1982) suggested that drought has a direct impact on apparition and acceleration of land degradation (water and wind erosion, salinization, etc.).

It also has an impact on rarefaction of natural vegetation which causes in return an important loss of soil. The highest progression rate of sand accumulations is recorded in the period 2000-2006, during which five of the seven years are dry, four of them are successive. The period 1975-1987 appears to be an episode of "equilibrium", during which, the progression rate is exactly equal to the regression rate. This suggests that the silting at this region is the result of a local remodeling: the amount of sand lost in areas of regression is regained at

Table 4. Change rates of Oglet Merteba (%).

Rate	1975-1987	1987-2000	2000-2006
C_g	9.8	9.9	9.3
C_a	0.82	0.76	1.54
P_a	0.41	0.44	0.77
R_a	0.41	0.32	0.78
P_{na}	0	0.12	-0.01

areas of accumulation of sand mapped as progression.

The same image processing software that we used to calculate change statistics allows automatic and spatial extract changes to occur between a time t_1 and an earlier time t_2 . Thus, for each time interval, a map could be generated showing in the legend:

1. Stable surfaces (which are always or always not silted sandy),
2. new sandy surfaces (pixels that exist only in time t_2),
3. and disappeared surfaces (pixels which existed in t_1 but not anymore in t_2).

The validation of these maps is a very difficult task because it relies only on the existing literature. Investigations made with the local population also helped to partially validate the results. Indeed, several factors (date of shooting, georeferencing error, failure of an instrument of shooting, shooting conditions, crop rotation) can cause considerable variations of spectral response and therefore can distort the results of changes.

The appearance of the central plain showed in the topographic map before 1975 does not seem to have a catastrophic dimension. Indeed, the difference images between 1975 and 1987 revealed that the extension of the sandy surface is more concentrated at the south-western study area in southern glacis of djebels. Newly sandy areas have more important dimensions down-stream

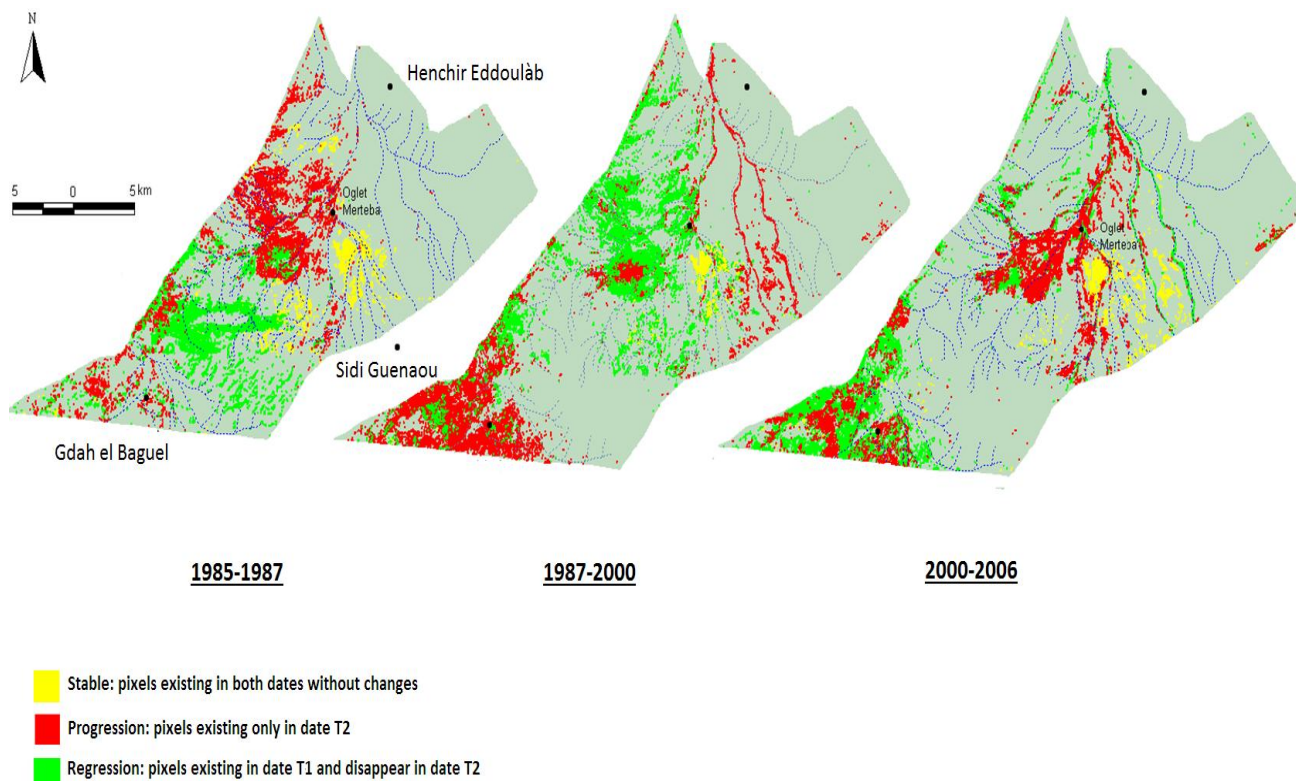


Figure 2. Spatial and temporal change of sandy surfaces.

Table 5. Change rates of Oglet Merteba (%).

Period	Wet years	Dry years	Trend	P_a	R_a	P_{na}
1975 - 1987	5	7 (with 3 successive)	Dry	0.41	0.41	0
1987 - 2000	4	10 (with 5 successive)	Dry, except 89-90 and 95-96 ^{oo}	0.44	0.32	0.12
2000 - 2006	2	5 (with 4 successive)	Dry	0.77	0.78	-0.01

stream. These glazes made in southern parts by limestone blocks, limestone and gypsum crusts developed on Mio-Pliocene sandy clays are cut by three main wadis (Ezzitoune wadis, Aissoub and Mguiltâ) that cause deflation of sandy sediments and their deposition in accumulation zones

In 2000, no changes were noticed at the west central part compared to 1987. On the contrary, we are witnessing the emergence of a very localized area of silting at the disposal of the Wadi el Oglet Merteba; thus constituting the downstream alluvial deposits. On the other hand, the complete erosion of the limestone of the short crust glazes through the many small wadis from Djebel Halouga locally because of the appearance of the gypsum crust.

Steppic vegetation developed in these areas promotes accumulation and deposition of sand and local redistribution. The dismantling of Jebel Elmalaâb by the same process of removal of Mio-Pliocene sandy clays causes scabbing gypsum which explains the negative changes noted in the given map (Pontanier and Zante, 1976).

Stable sand surfaces occupy a small area; they are located in the plain of Oglet Merteba and seem to evolve over the last map change near the village of Sidi Guenaou.

The appearance of the sandy plain from a time prior to the acquisition of the first image in the diachronic series and its extension does not seem to have a cata-strophic dimension.

Conclusion

This study shows that the integrated methodology using together segmentation technique for thresholds determination of “sand” and photo-interpretation for identification of sandy soils is useful to assess wind erosion dynamics through the mapping of the spatial and temporal evolution of sandy soil. According to these results, Oglat Merteba is more affected by sand accumulation over the last decade. The more aggressive period is noticed in 2006. These newly affected areas are located in the central plain zone.

REFERENCES

Adeel Z, Safriel U, Niemeijer D, Robin White (2005). Ecosystems and Human Well-being: Desertification Synthesis. A report of the Millennium Ecosystem Assessment. World Resources Institute, Washington, DC.

Bai ZG, Dent DL (2007). Land degradation and improvement in Tunisia. 1. Identification by remote sensing. Report 2007/08, ISRIC - World Soil Information, Wageningen

Bannari A, El-Harti A, Haboudane D, Bachaoui M, El-Ghmari A (2007). Intégration des variables spectrales et géomorphométriques dans un SIG pour la cartographie des zones exposées à l'érosion. *Revue Télédétection* 7(1-4):393-404

Chahbani B (1992). Dynamique des phénomènes éoliens et technique anti-Erosive dans les régions prédesertiques de la Tunisie. Thèse de doctorat. Faculté des sciences agronomiques de Gand-Belgique. pp. 180.

Deer PJ (1995). Digital change detection techniques: civilian and military applications. International Symposium on Spectral Sensing Research's 1995 Reports.

Escadafal R (1989). Caractérisation de la surface des sols arides par observations de terrain et par télédétection. Applications : Exemples de la région de Tataouine (Tunisie). Paris, thèse de doctorat. Univ. Paris VI. pp. 317.

Escadafal R, Belghit A, Ben-Moussa A (1994). Indices spectraux pour la télédétection de la dégradation des milieux naturels en Tunisie aride. P. 253-259, in G. Guyot (réd.) Actes du 6^{ème} Symposium international sur les mesures physiques et signatures en télédétection, Val d'Isère (France), 17-24 janvier 1994, ISPRS-CNES

Escadafal R, Huete AR (1991). Étude des propriétés spectrales des sols arides appliquée à l'amélioration des indices de végétation obtenus par télédétection. *Comptes-rendus de l'Académie des Sciences de Paris, Série* 312:1385-1391.

Floret C, Pontanier R (1982). L'aridité en Tunisie présaharienne. Climat, sol, végétation et aménagement. Travaux et documents de l'ORSTOM. N°150, Paris. pp. 544.

Fung T, Ledrew E (1987). The application of principal component analysis to change detection. *Photogramm. Eng. Remote Sens.* 53:1649-1658.

Ghram-Messedi A, Delaître E (2007). Les états de surface en zone aride à partir d'indices radiométriques et de classifications multitemporelles d'images Landsat TM prises sur la région de Menzel Habib (Tunisie méridionale). *Revue Sécheresse* 18(4):305-313.

Hayes DJ, Sader SA (2001). Comparison of Change Detection Techniques for Monitoring Tropical Forest Clearing and Vegetation Regrowth in a Time Series. *Photogramm. Eng. Remote Sens.* 67 (9):1067-1075

Jauffret S (2001). Validation et comparaison de divers indicateurs des changements à long terme dans les écosystèmes méditerranéens arides : Application au suivi de la désertification dans le Sud tunisien. Thèse univ. Aix Marseille. pp.372.

Jensen JR (2004). *Introductory digital image processing - a remote sensing perspective.* 3rd ed. Prentice Hall, Upper Saddle River (N.J.). pp. 316.

Jensen JR, Cowen D J, Althausen JD, Narumalani S and Weatherbee O (1993). An evaluation of the Coastwatch change detection protocol in South Carolina. *Photogramm. Eng. Remote Sens.* 59:1039-1046.

Lu D, Mausel P, Brondizio E, Moran E (2004). Change detection technique. *Int. J. Remote Sens.* 25 (12):2365-2407.

Mathieu R, Pouget M, Cervelle B, Escadafal R (1998). Relationships between satellite based radiometric indices simulated using laboratory reflectance data and typic soil color of an arid environment. *Remote Sens. Environ.* 66:17-28.

Mougenot B, Cailleu D (1995). Identification par télédétection des sols dégradés d'un domaine sahélien au Niger. Actes du Symposium International AISS (groupe de travail RS et DM), Ouagadougou, Burkina Faso, 6 au 10 février. pp. 169-179.

Ouaidrari H, Vermote E (1999). Operational Atmospheric Correction of Landsat TM data. *Remote Sens. Environ.* 70: 4-15

Querchefani D, Dhaou H, Abdeljaoued S, Delaire E, Callot Y (2009). Radiometric indices for monitoring soil surfaces in South Tunisia. *J. Arid Land Stud.* 19 (1):73-76.

Pontanier R, Zante P (1976). Etude pédologique de la zone d'Oglat-Merteba délégation d'El Hamma de Gabes. N° 507.

Talbi M (1993). Contribution à l'étude de la désertification par télédétection dans la Jeffara (Tunisie du Sud-Est). Doctorat de 3ème cycle en géographie. Faculté des Sciences Humaines et Sociales de Tunis. 2 tomes, pp. 305.

Vermote EF, Tanré D, JL Herman, Morcrette JJ (1997). Second Simulation of the Satellite Signal in the Solar spectrum, 6S: An Overview. *IEEE Trans. Geosci. Remote Sens.* 35 (3):675-686.